

Multichannel QRS Morphology Clustering

Data Preprocessing for Ultra-High-Frequency ECG Analysis

Filip Plesinger¹, Juraj Jurco¹, Josef Halamek¹, Pavel Leinveber², Tereza Reichlova² and Pavel Jurak¹

¹*Institute of Scientific Instruments of the Czech Academy of Sciences, Brno, Czech Republic*

²*International Clinical Research Center at St. Anne's University Hospital, Brno, Czech Republic*

Keywords: ECG, SAECG, QRS, Ultra-High-Frequency, Clustering, Multi-thread, Ventricle Dyssynchrony.

Abstract: Ultra-high-frequency ECG (UHF-ECG) in a range of 500–1,000 Hz has been tested as a new information source for analysis of left-ventricle dyssynchrony and other myocardial abnormalities. The power of UHF signals is extremely low, for which reason an averaging technique is used to improve signal-to-noise ratio. Since ventricle dyssynchrony is different for various QRS complex types, the detected QRS complexes must be clustered into morphology groups prior to averaging. Here, we present a fully-automated method for clustering. The first goal of the method is to separate previously detected QRS complexes into different morphology groups. The second goal is to precisely fit the QRS annotation marks to the exact same position against the QRS shape. The method is based on the Pearson correlation and is optimized for parallel processing. In our application with UHF-ECG data the number of detected groups was 3.24 ± 3.41 (mean and standard deviation over 1,030 records). The method can be used in other areas also where the clustering of repetitive signal formations is needed. For validation purposes, the method was tested on the MIT-BIH Arrhythmia and INCART databases from Physionet with results of purity of 98.24 % and 99.50 %.

1 INTRODUCTION

The electrocardiogram (Fig. 1A) is one of the most important sources of knowledge about heart function. The analyzed frequency band is mostly limited to 150 Hz. At higher frequencies the most limiting factor is the signal-to-noise ratio, which can be surpassed using the signal-averaged ECG (SAECG), suppressing noise thanks to averaging large number (over tens or more) of QRS complexes. Using SAECG, fetal QRSs were extracted from maternal ECG (Hon and Lee, 1963) and weak signals in frequency range 40-300 Hz revealed high-frequency QRS potentials (Goldberger et al., 1981). Moreover, SAECG technique allowed further research in the fields of ventricular late potentials (Simson 1983; Haberl et al. 1988; Jarrett and Flowers, 1991) and atrial fibrillation (Fukunami et al., 1991). Several devices for SAECG were developed in the past as ART 1200 EPX, Corazonix Predictor or VCM-3000.

But every step on this high-frequency road was laid into the range below 250-300 Hz, assuming that there is nothing useful above. It was correct for early times when bit-depth of common analog/digital

converters allowed 12 bits, dislodging weak potentials of higher frequencies into quantization darkness. Detection of Reduced Area Zones (RAZ) also uses the frequency range of 150-250 Hz (Abboud et al., 1987). Accessibility of this technique (later implemented in Hyper-Q devices) gained new research in myocardial ischemia (Schlegel et al., 2004), ECG during anesthesia (Spackman et al., 2005) or in myocardial infarction (Amit et al., 2013).

Even the spread of SAECG and continuously increased technical level of analog to digital converters both in sampling frequency and bit depth (note common 192 kHz and 24 bits in the field of digital audio recording), the clinical community still relies on well-proven frequency range of 0-150 Hz in classic ECG while only fearless specialists use RAZ analysis in high-frequency range 150-250 Hz (HF-ECG).

Against those habits, our team has developed and tested an innovative method for ultra-high-frequency ECG (UHF-ECG; up to 2 kHz) analysis (Jurak et al., 2013) that provides information about spatial and temporal distribution of depolarization phase of action potentials. Furthermore, it is able to reveal ventricle dyssynchrony with the common 12-lead

ECG that cardiology specialists are used to. As the preliminary results show, dyssynchrony can be derived from UHF signal envelopes in the QRS complex region in leads V1 and V6. A high-dynamic acquisition system must be used simultaneously with new processing methods to acquire UHF-ECG.

We have used input data with a sampling rate of 5 kHz and 24-bit dynamic range which allows us to analyze UHF envelopes in a frequency range of 500–1,000 Hz (Fig. 1B), being high above currently accepted frequency range. The power in this range is very weak; the QRS amplitude in the UHF envelope is approximately 80 dB lower than the low-frequency (up to 150 Hz) QRS complex amplitude (compare Figures 1A and B).

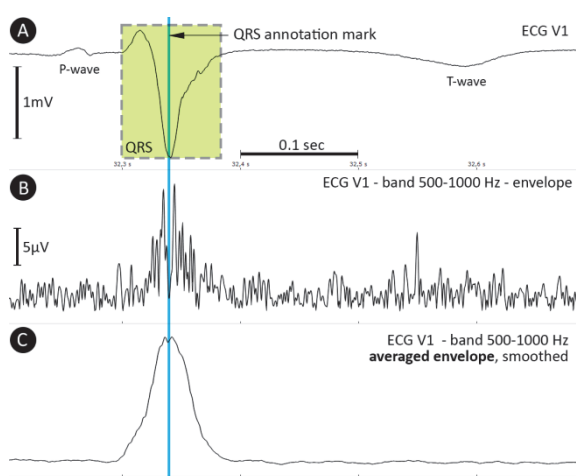


Figure 1: A – ECG signal with P-wave, QRS complex and T-wave; B – signal envelope in the 500–1,000 Hz band; C – averaged envelope, smoothed (40 samples, rectangular window).

Signal averaging (mentioned as SAECG before) is applied to increase the signal-to-noise ratio using QRS annotation marks as reference points. QRS complexes must be clustered into groups specified by QRS morphology due to the possible presence of more beat types within a single ECG record.

Furthermore, QRS annotation marks must point to exactly the same sample (Rompelman and Ros, 1986a; Rompelman and Ros, 1986b) inside the QRS shape (Fig. 1A). Envelopes in the range 500–1,000 Hz (Fig. 1C) can then be averaged using tens to hundreds of beats depending on the signal quality. The electrical activity of the myocardium, expressed by UHF-ECG envelopes, carries specific temporal and spatial information that can be further analyzed (Jurak et al., 2013).

The clustering process is, therefore, an essential step in UHF-ECG analysis as it is needed to assure

that UHF envelopes belonging to different QRS types will not be mixed together during averaging. A similar need has been described in a study (Amit et al., 2013) before averaging the signal to obtain RAZ.

Current clustering methods (Castro and Paulo, 2014; Lagerholm and Peterson, 2000; Cuesta-Frau et al., 2003; Chang et al., 2005) aim to assign previously detected QRS to known beat types. This goal is not sufficient for our objective due to the fact that a specific beat type may have different morphologies (leading to different UHF-ECG envelopes) which have to be distinguished. Also, existing approaches do not correct the positions of QRS annotation marks which is an important step to maintain detail in averaged envelopes.

We are, therefore, proposing a new clustering method that can be used in UHF-ECG analysis and works with multiple leads without human intervention, allowing full automation.

2 METHOD

2.1 Method Inputs and Preprocessing

The mounted signals from ECG V-leads (V1 to V6) and a list of QRS annotations are inputs for the method. QRS annotations are acquired by a robust multi-lead detection method (Plesinger et al., 2014) and cleared of pacemaker activity. Thus, only signal preprocessing steps are mounting and pacemaker activity removal, where areas influenced by pacemaker activity are replaced by the linear interpolation.

2.2 Processing

Processing is presented in a flowchart (Fig. 2).

2.2.1 Primary Clustering

At the beginning (Fig. 2A), the first QRS annotation is declared the first member of the first morphology group. Next, the segment around the first unassigned QRS annotation is compared by Pearson correlation to each of the QRS annotations already assigned. This is performed simultaneously (as a multi-thread process) in leads V1 to V6 within an area of ± 120 ms around the QRS annotation and six correlation coefficients are obtained. If the lowest correlation coefficient C_{\min} is higher than correlation threshold C_t , the unassigned QRS is linked to the group of correlating QRS annotation. If the tested QRS annotation cannot be assigned to any of the existing

morphology groups, a new group is created and the unassigned QRS is linked to it as its first member. This loop is repeated until none of the QRS annotations remains unassigned.

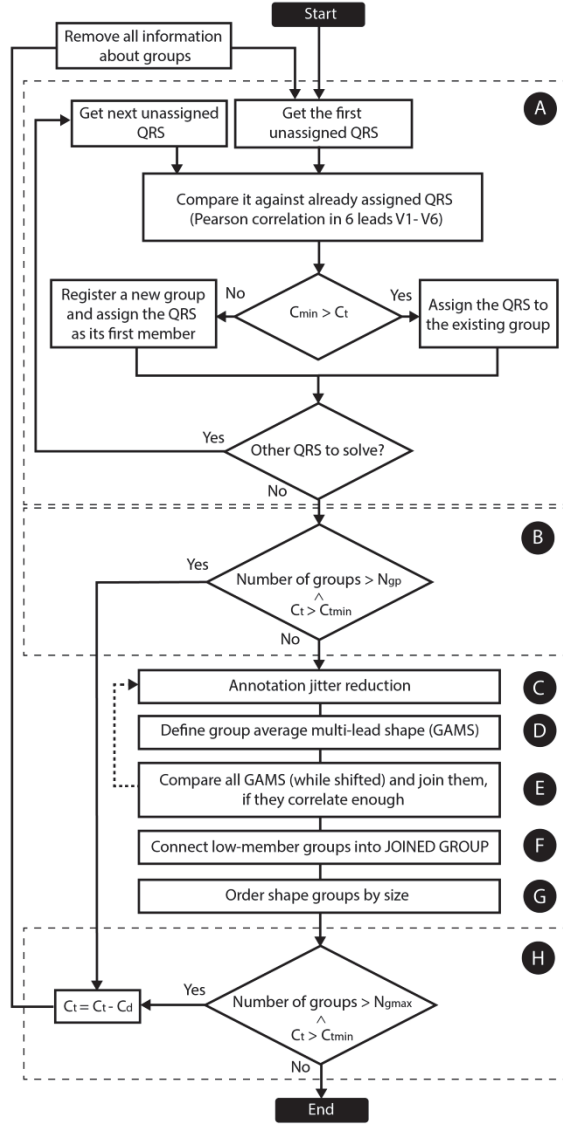


Figure 2: Method flowchart. A – primary clustering, B – correlation threshold reduction, C – annotation jitter reduction, D – computation of averaged shapes, E – shift-test, F – connecting small groups into a joined group, G – group reordering, H – group count check. C_{min} is the lowest correlation from leads V1 to V6, C_t is the current corr. threshold (0.98 at the beginning of the process), C_{tmin} the minimal permitted correlation threshold (0.75), C_d the decrement of the correlation threshold, N_{gp} the maximum number of groups permitted after primary clustering, N_{gmax} the maximum number of groups.

2.2.2 Annotation Jitter Reduction

QRS annotations inside each morphology group must be exactly aligned with one another. The highest correlation between each QRS segment (leads V1 to V6) and the first member of each group is found by shifting the QRS annotation to the left and right (Fig. 1C).

2.2.3 Group Average Multi-lead Shapes

A group average multi-lead shape (GAMS) is created (Fig. 2D and Fig. 3C) for each morphology group by averaging corresponding samples from all QRS complexes from the specific group. Each GAMS contains six averaged shapes (leads V1-V6).

2.2.4 Group Shift-test

It is possible that two or more groups contain a similar type of QRS morphology, merely shifted to the left or right. To merge such groups together, the central part (a width of 120 ms) of each GAMS is correlated with the GAMS of other groups when shifted to the left and right (Fig. 2E). If the correlation maximum is higher than threshold C_{ts} , the groups are joined together and the program jumps back to the jitter reduction (Fig. 2C).

2.2.5 Joined Group

Groups containing less than three QRS annotations are assigned to the “Joined Group” (Fig. 2F and Fig. 3 – the last column). This usually contains misidentified QRS annotations and artefacts. A large Joined Group can be produced if the source is too noisy.

2.2.6 Order Groups by Size

Next, the shape groups are arranged by the number of related QRS annotations except the Joined Group (Fig. 2G). The shape group with the largest number of QRS is named Group 1, the second Group 2 etc.

2.2.7 Check Groups Count

If the number of groups is still too high (>50) and C_t is higher than C_{tmin} , correlation threshold C_t is decreased and the computation is restarted (Fig. 2H).

2.3 Method Outputs

The method produces a modified QRS annotations list, where each of the QRS annotations retains the

information identifying the morphology group to which a specific QRS belongs. Information about the location of each QRS is updated when the offset correction and group shift-test tasks (Fig. 2C and 2E) are completed. Statistical properties providing information about the correlation between GAMS and each member of a specific group are also saved for statistical processing.

3 RESULTS

3.1 Application

The source data for our method are records 8–15 minutes long in a resting supine position; sampling rate 5 kHz and bit resolution 26 bits (25 kHz and 24 bits before down-sampling). This dataset (UHF-ECG) has been recorded at the International Clinical Research Center at St. Anne’s University Hospital, Brno, Czech Republic using a recording device from the company M&I, Prague. A total number of 1,030 recordings have been made (262 ischemic heart disease, 36 hypertrophic cardiomyopathy, 302 dilated cardiomyopathy, 261 heart transplant and 169 healthy subjects).

Using the presented method, all the available records were clustered into morphology groups with an average number of groups per record of 3.24 ± 3.41 . The average percentage of QRS assigned to the “Joined Group” (the group of QRS which did not correlate well enough with any of the other groups) was $0.99 \% \pm 2.09$ and the average percentage of QRS in Group 1 was $95.42 \% \pm 9.85$. The median correlation between each member of the majority group (Group 1) and the corresponding averaged shape was 0.997 ± 0.005 (over 1030 records). Overall results for UHF-ECG dataset are shown in Table 1.

Table 1: UHF-ECG dataset results. G1 - amount of QRS in largest group, JG - amount of QRS in Joined Group, Ng – number of detected groups.

	Med.	Mean \pm SD	Min	Max
G1 [%]	99.51	95.37 ± 9.94	24.54	100.0
JG [%]	0.25	0.99 ± 2.11	0.00	27.65
Ng	2.00	3.27 ± 3.45	1.00	39.00

The application is presented in Fig. 3 on a subject with dilated cardiomyopathy. QRS complexes were detected from a 12-lead UHF-ECG record (Fig. 3A) and clustered using leads V1 to V6 into five morphology groups (Fig. 3B). The majority

group – Group 1 – (Fig. 3B, the first column and Fig. 4A) contains 711 QRS. The second group (Fig. 4B) contains 235 QRS. Group 3 and Group 4 (not displayed) contains only 27 and 4 QRS, for which reason it is not usable for averaging.

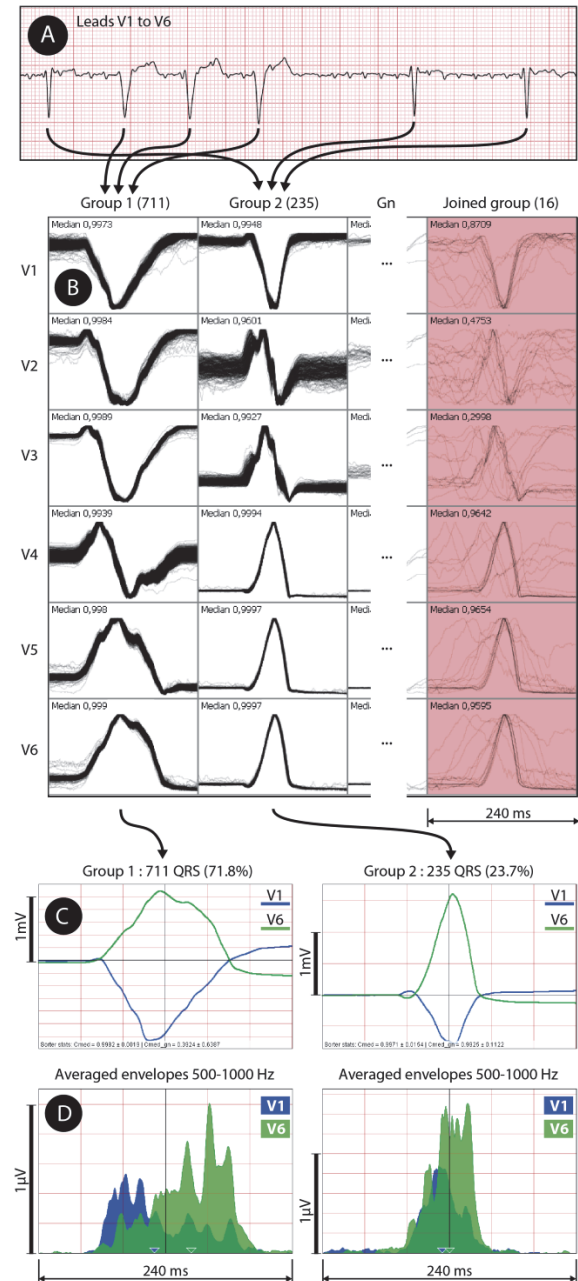


Figure 3: Method application: A – raw ECG data, B – clustering method result (clusters in columns, leads in rows) with median correlation inside each cell, C – averaged QRS shapes for two largest groups, D – averaged envelopes in range 500–1,000 Hz for two largest QRS groups. UHF-ECG subject 0766.

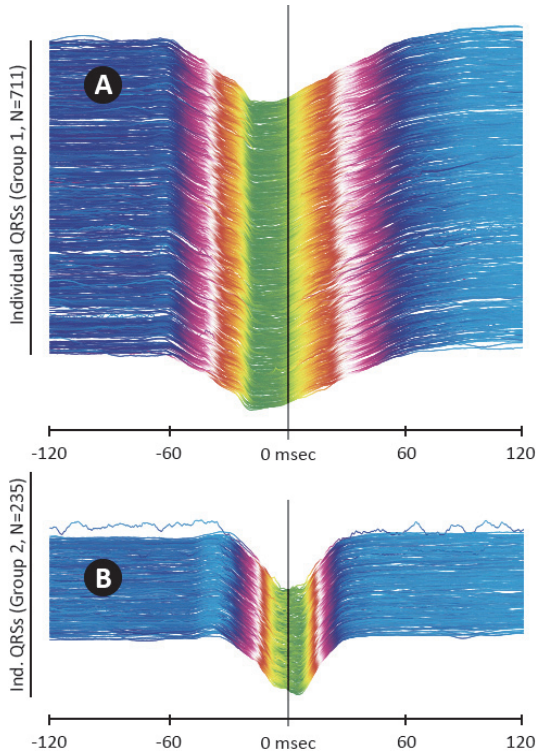


Figure 4: Categorized QRS complexes, ECG V1 lead in 240 ms window. A – Group 1 QRS complexes, B – Group 2 QRS complexes. Vertical line in the middle shows QRS annotation mark (i.e. trigger). UHF-ECG subject 0766.

The “Joined Group” (Fig. 3B, the last red column) contains 16 QRS which were not attached to any of the existing groups due to noise or artefacts. Each cell in the grid (Fig. 3B) contains a 240-millisecond-long window and each drawn QRS is normalized to fill the predefined height of the cell (i.e. auto-scaled). Once QRS complexes are clustered into groups, it is possible to compute and average amplitude envelopes in a range of 500–1,000 Hz using FFT and Hilbert transform. The averaged envelopes for Group 1 and Group 2 are shown in Fig. 3D. In comparison with the greatly magnified averaged QRS shape of Group 1 (Fig. 3C), we can see large electrical dyssynchrony revealed between leads V1 and V6 (Fig. 3D).

3.2 Method Validation using Physionet Annotated Databases

The MIT-BIH Arrhythmia (Moody and Mark, 2001) and INCART databases from Physionet (Goldberger et al., 2000) were used with 47 and 75 records, respectively, for validation and comparison purposes. The data quality does not allow the use of these databases for UHF-ECG analysis (the

sampling rate and bit resolution are insufficient), but they are carefully annotated by specialists and existing QRS annotations can be used to evaluate the purity of the clustered groups.

Specificity and sensitivity values or confusion matrixes (usual ways to validate clustering method) could not be computed because the presented method does not aim to cluster QRS by any known pathological morphology. Instead, purity (P) values for both databases were computed to show the level of contamination of clustered groups by different QRS types (defined in Physionet beat annotations). P was computed over all subjects and groups (except for Joined Groups) as:

$$P = 100 - 100 \times \frac{\sum_{all\ groups} (N_{QRS} - N_{major})}{N_{total}} \quad (1)$$

where N_{QRS} is the number of all QRS complexes within the specific group, N_{major} is the maximal occurrence of any beat type (specified by Physionet annotations) in the specific group, and N_{total} is the sum of all QRS over all subjects and groups (except for Joined Groups). The overall purity of MIT-BIH was 96.69 % and 98.38 % for the INCART database. Purity can also be evaluated separately for each subject/record and Tables 2 and 3 show purity, group sizes and group count statistics for the MIT-BIH and INCART databases.

Table 2: Results for MIT-BIH arrhythmia database records. P – purity, G1 - amount of QRS in the largest group, JG - amount of QRS in Joined Group, Ng – number of detected groups.

	Med.	Mean \pm SD	Min.	Max.
P [%]	99.84	96.87 \pm 8.26	51.15	100
G1 [%]	79.41	79.23 \pm 16.39	28.68	99.41
JG [%]	4.13	9.09 \pm 9.63	0.20	31.03
Ng	18.00	23.77 \pm 17.89	2.00	70.00

Table 3: Results for INCART database records.

	Med.	Mean \pm SD	Min.	Max.
P [%]	99.95	98.47 \pm 4.98	69.21	100
G1 [%]	73.92	75.09 \pm 17.01	35.24	99.59
JG [%]	3.82	7.87 \pm 8.68	0.00	33.48
Ng	13.50	19.29 \pm 15.38	2.00	71.00

The overall purity of MIT-BIH was 96.69 % and 98.38 % for the INCART database, meaning that the resultant groups are slightly contaminated by different beat types. Further insight into the contamination issue showed it is possibly caused by two reasons:

First, our method is not able to distinguish between premature and escape beats having the same shape as another QRS type (i.e. atrial premature beats – A – and normal sinus beats – N – in record 202 in MIT-BIH). Joining these beats together (which is acceptable for our goals) will increase average purity to 98.24 % (MIT-BIH) and 99.50 % (INCART).

Second, due to noise, individual shapes are not able to correlate enough with existing morphology groups and a large number of groups can be created. If the number of groups is too high, the correlation threshold can be decreased which may lead to the unwanted linking of different beat types into one group (as in the case of records 208 and 213 from MIT-BIH).

Another issue can occur when the bottom limit to correlation threshold (0.75) is met, but it is not possible to create larger groups ($N_{QRS} > 3$). In this way, the majority of QRS are moved to the Joined Group (as in records 2, 3 and 58 from INCART).

3.2.1 Results Comparison

Specific results for validation records are presented by Table 4 (MIT-BIH), showing comparison values for groups detected by our method and an existing method (Castro and Paulo, 2014).

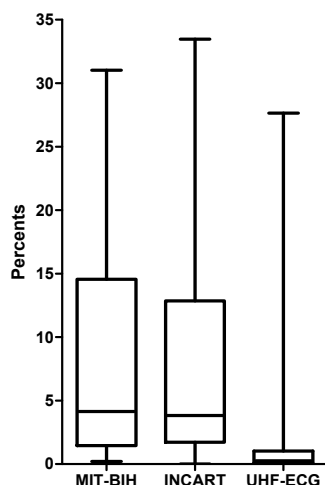


Figure 5: Joined Group sizes for two Physionet databases and UHF-ECG dataset. Medians 4.13 (MIT-BIH), 3.82 (INCART) and 0.26 (UHF-ECG).

The number of QRS complexes in Joined Groups (Fig. 5) indicates how many QRS complexes are not (hypothetically) suitable for the following UHF-ECG analysis. This value should be as low as possible. The number of groups generated by clustering (Fig. 6) is lowest for the UHF-ECG

database, though it strongly depends on subject-specific pathology as well as signal quality.

Table 4: Results for MIT-BIH database records. P – purity, G1 – amount of QRS in Group 1, JG – amount of QRS in Joined Group, N_g – number of groups generated by our method, N_{gc} – number of groups generated by compared method (Castro and Paulo, 2014).

Record	P [%]	G1 [%]	JG [%]	N_g	N_{gc}
100	98.58	99.34	0.66	2	4
101	99.86	68.47	23.43	52	4
102	99.86	92.36	1.28	17	10
103	100.00	85.94	7.20	29	10
104	98.77	56.98	15.84	54	16
105	100.00	68.23	26.87	28	10
106	100.00	44.89	30.93	30	27
107	100.00	96.40	0.94	10	11
108	99.70	60.64	25.47	18	22
109	100.00	97.08	1.70	7	13
111	100.00	90.58	6.54	17	8
112	99.96	82.63	8.00	39	4
113	100.00	96.99	1.06	10	5
114	99.58	66.58	11.66	70	8
115	100.00	97.75	1.54	8	11
116	99.96	92.91	2.99	13	10
117	99.93	99.41	0.59	2	4
118	95.84	93.81	3.86	13	3
119	100.00	77.45	0.20	3	6
121	99.94	95.60	4.13	4	5
122	100.00	82.96	9.37	55	1
123	100.00	99.41	0.26	4	3
124	98.10	53.24	2.66	16	14
200	96.99	28.68	31.03	48	20
201	97.95	84.11	3.16	11	15
202	98.62	96.77	1.45	9	9
203	99.50	62.08	26.31	43	33
205	99.92	79.07	6.81	49	14
207	94.92	79.41	6.94	22	61
208	51.15	67.11	29.48	32	28
209	90.34	71.11	27.29	20	10
210	100.00	79.70	11.32	39	27
212	100.00	66.05	14.56	38	5
213	81.83	98.40	1.32	5	17
214	99.95	87.75	2.61	13	21
215	99.96	76.06	17.45	38	16
217	98.82	70.15	4.08	30	28
219	99.63	96.75	0.56	7	14
220	95.62	98.88	0.83	4	2
221	100.00	61.27	18.34	34	14
222	83.68	73.66	12.12	64	8
223	96.57	79.31	3.72	21	23
228	99.84	65.76	9.40	25	14
230	100.00	58.07	1.68	8	3
231	99.87	79.31	1.08	12	5
232	77.76	92.47	5.79	15	4
233	99.67	72.04	2.60	29	24

A comparison of the results from the UHF-ECG dataset and MIT-BIH and INCART databases in Figure 5 shows that data quality greatly influences the number of unsuccessfully clustered beats.

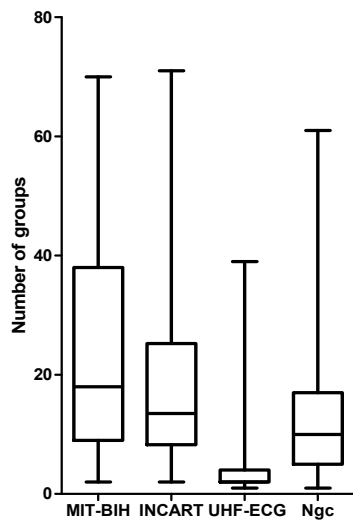


Figure 6: Comparison of number of group count results for MIT-BIH (median 18), INCART (median 13.5), UHF-ECG dataset (median 2) using the presented method and MIT-BIH results (median 10) acquired from (Castro & Paulo 2014) as the last bar - Ngc.

4 DISCUSSION

The proposed method is able to categorize QRS (Fig. 7) in high sampled data (5,000 Hz) and great bit-depth (26 bits), allowing to see ultra-high frequency potentials in individual morphology groups and able to reveal ventricle dyssynchrony as in Fig. 3. Thanks to the direct comparison among all of registered QRS this method is able to catch continuous changes in QRS morphology (which we encountered while detecting QRS from isolated hearts).

This is in contrast to building of morphology template (Breithardt et al., 1991). On the other hand, due to this behavior the processing time increases to uncomfortable lengths while processing long (hours) UHF-ECG recordings.

Figure 7 presents method results, showing temporal distribution of detected morphology groups in part of 15-minute record. Such technique may be used even for standard 6-12 leads ECG.

The legitimacy of using frequencies above usual 300 Hz is shown in Figure 8. Even the currently used HF frequency range of 150-250 Hz (Fig. 8B) shows dyssynchrony of specific QRS, it is obvious that frequency range of 500-1,000 Hz (Fig. 8C) provides more precise image of ventricles electrical activation with higher temporal resolution. On the other hand, range of 1,000-2,000 Hz (Fig. 8D) brings less evident activity due to significantly lower

signal-to-noise ratio.

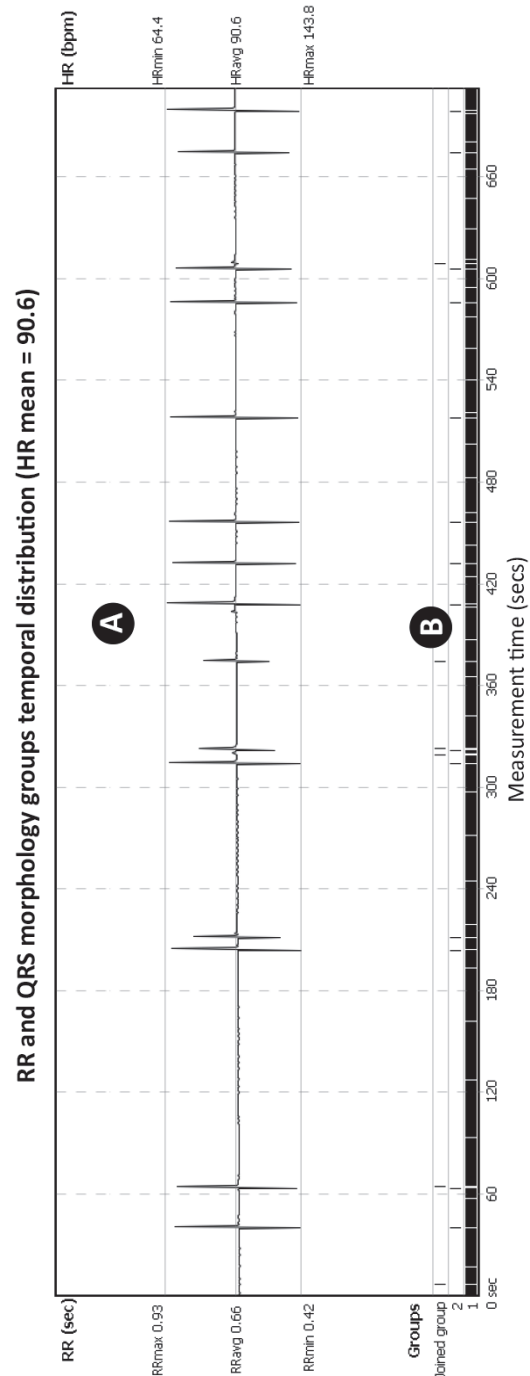


Figure 7: Temporal distribution of QRS morphology groups during the measurement of heart-transplant subject (UHF-ECG subject 0086). A – RR intervals (beat-to-beat) excluding beats from Joined Group, B – morphology groups temporal distribution, where Group 1 (major occurrence) is a normal QRS, rarely interrupted with ventricle beats from Group 2. Unrecognized or false positive QRS complexes are in Joined Group.

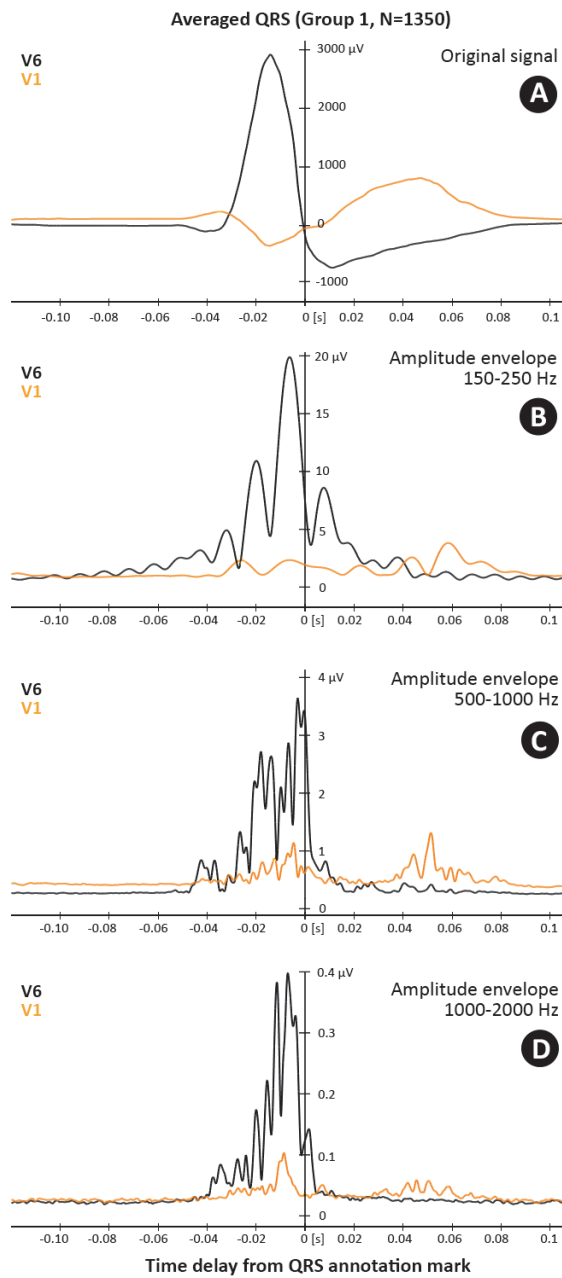


Figure 8: Comparison of averaged QRS shape (N=1350) in different frequency ranges for leads V1 (orange) and V6 (black). Only QRSs from Group 1 were taken into account. A – averaged QRS complex, B – amplitude envelopes in 150-250 Hz, C – amplitude envelopes in 500-1,000 Hz, D – amplitude envelopes in 1,000-2,000 Hz (UHF-ECG subject 0086).

Two Physionet databases (MIT-BIH and INCART) were processed to validate the presented clustering method and the purity of the clustered QRS groups was 98.24 % (MIT-BIH) and 99.50 % (INCART), respectively. This purity shows the level

of correspondence between annotated QRS types and clustered groups. The median correlation within Group 1 for the UHF-ECG dataset was 0.997, showing extremely high overall morphology stability inside the majority group. In comparison with an existing clustering method (Castro and Paulo, 2014) in Fig. 6 and Table 4, our approach produces a larger number of groups (the median from the N_g column is 18, while the median from N_{gc} is 10).

Although the method is designed to work with specific UHF-ECG data, it can be used in any other area where the clustering of repetitive signal formations according to shape is needed (as shown in figure 9 with P-wave example).

5 CONCLUSIONS

A multichannel clustering method has been presented as an essential part of UHF-ECG analysis. The method clusters a list of previously detected QRS complexes into groups by morphology and corrects QRS annotation mark positions inside each group to point to exactly the same location of QRS shape. This functionality allows averaging of UHF-ECG envelopes with regard to specific QRS types and, thanks to annotation jitter reduction, the averaged UHF envelopes retain the highest possible amount of detail. Correctly averaged UHF-ECG envelopes are tested by a related study to reveal information on heart ventricle dyssynchrony.

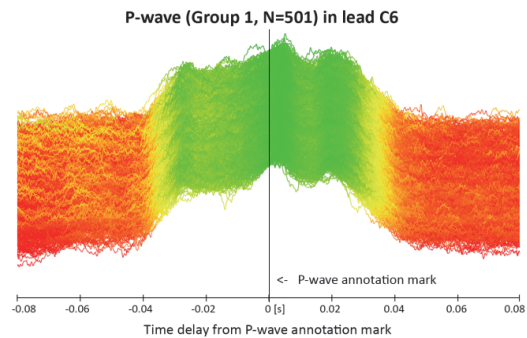


Figure 9: Presented clustering method used for clustering of P-wave. 538 P-waves total, 501 were clustered into Group 1 and 37 into Joined Group. UHF-ECG subject 0616 with dilated cardiomyopathy.

It is also evident that our method works significantly better with the UHF-ECG dataset (for which the method was originally designed) than with low-resolution data from the MIT-BIH and INCART databases.

The presented method is part of the software UHF Solver which is used for autonomous processing of UHF-ECG data to obtain information about heart ventricle dyssynchrony. Also, the method has been implemented as a plugin for SignalPlant, free signal-processing and visualization software.

ACKNOWLEDGEMENTS

This research was supported by project no. P102/12/2034 from the Grant Agency of the Czech Republic and by MEYS CR (LO1212), its infrastructure by MEYS CR and EC (CZ.1.05/2.1.00/01.0017) and by ASCR (RVO: 68081731).

REFERENCES

- Abboud, S. et al., 1987. Detection of transient myocardial ischemia by computer analysis of standard and signal-averaged high-frequency electrocardiograms in patients undergoing percutaneous transluminal coronary angioplasty. *Circulation*, 76(3), pp.585–596.
- Amit, G. et al., 2013. High-frequency QRS analysis in patients with acute myocardial infarction: a preliminary study. *Annals of noninvasive electrocardiology: the official journal of the International Society for Holter and Noninvasive Electrocardiology, Inc*, 18(2), pp.149–156.
- Breithardt, G. et al., 1991. Standards for analysis of ventricular late potentials using high-resolution or signal-averaged electrocardiography. A statement by a Task Force Committee of the European Society of Cardiology, the American Heart Association, and the American College of Ca. *Circulation*, 83(4), pp.1481–1488.
- Castro, D. & Paulo, F., 2014. A method for context-based adaptive QRS clustering in real-time. *Biomedical and Health Informatics, IEEE Journal of*, PP(99), pp.1–12.
- Cuesta-Frau, D., Pérez-Cortés, J. C. & Andreu-García, G., 2003. Clustering of electrocardiograph signals in computer-aided Holter analysis. *Computer Methods and Programs in Biomedicine*, 72(3), pp.179–196.
- Fukunami, M. et al., 1991. Detection of patients at risk for paroxysmal atrial fibrillation during sinus rhythm by P wave-triggered signal-averaged electrocardiogram. *Circulation*, 83(1), pp.162–169.
- Goldberger, A. L. et al., 1981. Effect of myocardial infarction on high-frequency QRS potentials. *Circulation*, 64(1), pp.34–42.
- Goldberger, A. L. et al., 2000. PhysioBank, PhysioToolkit, and PhysioNet: Components of a New Research Resource for Complex Physiologic Signals. *Circulation*, 101(23), pp.215–220.
- Haberl, R. et al., 1988. Comparison of frequency and time domain analysis of the signal-averaged electrocardiogram in patients with ventricular tachycardia and coronary artery disease: methodologic validation and clinical relevance. *Journal of the American College of Cardiology*, 12(1), pp.150–158.
- Hon, E. H. & Lee, S. T., 1963. Noise reduction in fetal electrocardiography. *American Journal of Obstetrics & Gynecology*, 87(8), pp.1086–1096. Available at: [http://dx.doi.org/10.1016/0002-9378\(63\)90104-2](http://dx.doi.org/10.1016/0002-9378(63)90104-2).
- Chang, K.-C. et al., 2005. A Comparison of Similarity Measures for Clustering of Qrs Complexes. *Biomedical Engineering: Applications, Basis and Communications*, 17(06), pp.324–331.
- Jarrett, J. R. & Flowers, N. C., 1991. Electrophysiology, Pacing, and Arrhythmia Signal-Averaged Electrocardiography: History, Techniques, and Clinical Applications. *Clin. Cardiol.*, 14, pp.984–994.
- Jurak, P. et al., 2013. Ultra-high-frequency ECG Measurement Institute of Scientific Instruments, AS, Brno, Czech Republic. *Computing in Cardiology Conference (CinC), 2013*, 40, pp.783–786.
- Lagerholm, M. & Peterson, G., 2000. Clustering ECG complexes using hermite functions and self-organizing maps. *IEEE Transactions on Biomedical Engineering*, 47(7), pp.838–848.
- Moody, G. B. & Mark, R. G., 2001. The impact of the MIT-BIH arrhythmia database. *IEEE Engineering in Medicine and Biology Magazine*, 20(3), pp.45–50.
- Plesinger, F. et al., 2014. Robust Multichannel QRS Detection. *Computing in Cardiology Conference (CinC), 2014*, 41, pp.557–560.
- Rompelman, O. & Ros, H. H., 1986a. Coherent averaging technique: a tutorial review. Part 1: Noise reduction and the equivalent filter. *Journal of biomedical engineering*, 8(1), pp.24–29.
- Rompelman, O. & Ros, H. H., 1986b. Coherent averaging technique: a tutorial review. Part 2: Trigger jitter, overlapping responses and non-periodic stimulation. *Journal of biomedical engineering*, 8(1), pp.30–35.
- Schlegel, T. T. et al., 2004. Real-time 12-lead high-frequency QRS electrocardiography for enhanced detection of myocardial ischemia and coronary artery disease. *Mayo Clinic proceedings. Mayo Clinic*, 79(3), pp.339–350.
- Simson, M. B., 1983. Clinical application of signal averaging. *Cardiol Clin*, 1(1), pp.109–119. Available at: <http://www.ncbi.nlm.nih.gov/pubmed/6399988>.
- Spackman, T. N., Abel, M. D. & Schlegel, T. T., 2005. Twelve-lead high-frequency QRS electrocardiography during anesthesia in healthy subjects. *Anesthesia and Analgesia*, 100(4), pp.1043–1047.